Available online at www.sciencedirect.com
ScienceDirect
Journal of Power Sources 163 (2007) 1114–1119
JOURNAL OF POWER SOURCES
www.elsevier.com/locate/jpowsour

Short communication

Chemical and electrochemical recycling of the negative electrodes from spent Ni–Cd batteries

M.B.J.G. Freitas *, T.R. Penha, S. Sirtoli

Universidade Federal do Espírito Santo, Departamento de Química, Laboratório de Eletroquímica Aplicada, Av. Fernando Ferrari s/n, Goiabeiras, Vitória-ES, CEP: 29060-900, Brazil

Received 2 August 2006; received in revised form 27 September 2006; accepted 29 September 2006
Available online 17 November 2006

Abstract

In this work, cadmium from Ni–Cd batteries was recycled by chemical precipitation and electrodeposition. Cadmium hydroxide, the material synthesized by chemical precipitation, showed up a hexagonal structure. The structure of the material recovered by chemical precipitation is not affected by the change of temperature at the range between 8.0 and 25 °C. The chemical composition for cadmium hydroxide is: [β-$Cd(OH)_2(H_2O)_X(SO_4)_Y(CO_3)_Z$] where *X*, *U*, and *W* are the amounts of substance for H_2O, SO_4^{2-}, and CO_3^{2-}, respectively.

Electrodepositing was accomplished using the galvanostatic technique. The chronopotentiometric plots present a potential peak that indicates a nucleation stage prior to deposit growth. The largest charge efficiency occurred around 95.0% for a current density between 10.0 and 30.0 mA cm^{-2}. Current density influences the morphology of the deposits. For a current density equal to 10.0 mA cm^{-2}, the deposit micro porosity is larger than that for a current density equal to 50.0 mA cm^{-2}. The deposits formed with current density of 25.0 mA cm^{-2} possess an intermediate morphology. The energy dispersive X-ray analysis (EDX) spectra of the deposits formed by different current densities have shown the presence of iron, sulphur, and oxygen besides cadmium.

Keywords: Recycling; Cadmium; Ni–Cd batteries

1. Introduction

The production of nickel–cadmium (Ni–Cd) batteries began in Europe and in the United States in 1950, soon after the development of the technology of stamped batteries by Neumann in 1940. As Ni–Cd batteries present environmental problems due to the presence of cadmium, other types of batteries have been developed. Nickel metal hydrate (NiMH) batteries are acceptable in environmental terms, and technically they can substitute Ni–Cd ones in many applications. Ion–lithium batteries are also produced as an alternative for Ni–Cd battery. Lithium and NiMH batteries are newer and more expensive than Ni–Cd batteries. Ni–Cd batteries are also used due to their great stability regarding to their capacity. Therefore, this battery type is largely used in precision fail-safe electronic equipment such as in medical and aviation devices [1–5].

The material found in the negative Ni–Cd electrode batteries from the discharge is the cadmium hydroxide, which showed three distinct phases: α-$Cd(OH)_2$, β-$Cd(OH)_2$ or γ-$Cd(OH)_2$. However, the main phase found on the negative electrode is β-$Cd(OH)_2$. This structure did not present hydrogen bonds for the crystal. The γ-$Cd(OH)_2$ presents a three-dimensional structure involving hydrogen bonds. The cadmium oxidation that produces the β-$Cd(OH)_2$ or γ-$Cd(OH)_2$ structure occurs on the same potential, independent of which of them is produced. α-$Cd(OH)_2$ is the least stable phase among all the hydroxides; consequently, it converts itself on β-$Cd(OH)_2$ structure fast [6].

When worn off, Ni–Cd batteries become dangerous residues. Therefore, they should be segregated, stored, treated, and disposed properly. The earth crust concentration of cadmium varies from 0.15 to 0.20 ppm. It is used in fungicide, battery, pigment production, and in surface coating [7]. Another way of reducing the cadmium's environmental impact is developing the recycling processes. Battery incineration would be a possible solution; however, this process is extremely hazardous to the environment as a large part of the metals evaporates, is released

* Corresponding author. Tel.: +55 27 33352486; fax: +55 27 33352460.
E-mail address: marcosbj@hotmail.com (M.B.J.G. Freitas).

0378-7753/$ – see front matter © 2006 Elsevier B.V. All rights reserved.
doi:10.1016/j.jpowsour.2006.09.087

into the atmosphere, and contaminates distant areas. Another means of recycling batteries is the hydrometallurgical process. It does not pollute the environment and can be easily applied at industrial scale [8–13]. Hydrometallurgical process of the spent Ni–Cd, Ni–MH, Zn–MnO_2, and ion–lithium batteries is a research line developed at the laboratory of applied electrochemistry. The characterization of negative electrodes from spent Ni–Cd batteries was discussed in the previous paper [14]. In this work, cadmium from Ni–Cd batteries was recycled by chemical precipitation and electrodeposition. Cadmium hydroxide was recovered by chemical precipitation adding NaOH 1.0 mol l^{-1} to the leaching solution. In the electrodeposition, cadmium was deposited onto steel 1020 by galvanostatic technique. The relationship between current density, charge efficiency, and deposit morphology was analyzed. The materials were characterized by X-ray diffraction (XRD), thermogravimetric analyses (TGA), thermodifferential analyses, Fourier transformation infrared spectroscopy (FT-IR), scanning electronic microscopy (SEM), and energy dispersive X-ray analysis (EDX).

2. Experimental

Battery recycling requires conditions of selective collection, disassembly, and a sequence of physical and electrochemical transformations. In the selective collection, worn out batteries are classified in homogeneous lots. Worn out AA Ni–Cd-type batteries produced by Toshiba (3.6 V, 600 mAh) were used in this research. In the disassembly, those batteries were physically separated in their different parts: anode, cathode, steel, separators, and current collectors. On an average, the weight of Ni–Cd battery parts corresponds to anode 25%, cathode 34%, and steel, separators, and current collectors 41% of the total.

2.1. Dissolution of cadmium electrodes

Anode dissolution accomplished with a solution of H_2SO_4, 0.5 mol l^{-1} in this condition was 1.000 g of anode material per 100 ml of H_2SO_4 0.5 mol l^{-1}. The suspension was maintained under constant stirring at 25 °C. After the dissolution of cadmium hydroxide, the current collector was removed from the solution and the suspension was filtered. The pH and the conductivity of the leaching solution were equal to 0.571 and 362.2 mS cm^2 mol^{-1}, respectively.

2.2. Cadmium hydroxide synthesis

The precursor material was obtained by chemical precipitation at 8 and 25 °C. The synthesis was carried out as follows: a solution of NaOH 0.500 mol l^{-1} was added by dripping on the 50.0 ml of the cadmium leaching solution at the rate of 10.0 ml min^{-1}. The suspension was under constant stirring. The precipitation of cadmium hydroxide happened with the addition of 90.0 ml of NaOH. The precipitate was filtered and washed with distilled water in order to remove the excess reagent. To an aliquot of the wash water was added a solution of $BaCl_2$ 1.000 mol l^{-1} until there was no more precipitation of $BaSO_4$. The mass of cadmium hydroxide obtained in the synthesis is equal to 0.6679 g for each 1.0006 g of the negative electrode.

2.3. Electrochemical cell

The work electrode was made by steel 1020 and coated with resin to isolate the part of the electrode where deposition would happen. The area obtained was 0.2 cm^2. The surface was sanded with 600-grit sandpaper to remove the product of iron oxidation. The auxiliary electrode was a platinum piece with geometric area of 3.75 cm^2. The reference electrode was Ag/AgCl saturated with NaCl. Before each electrochemical experiment, the working electrodes were sanded with 600-grit sandpaper and then rinsed with distilled water. Galvanostatic experiments were performed with a laboratory-built regulated power supply. Work and auxiliary electrodes were connected to the voltmeter and to a microcomputer through an RS232 interface. The electrolyte solutions were prepared with reagent p.a. and pure water. Solutions were changed after each experiment. All electrochemical experiments were performed at 298 K.

The charge density used was 90.0 C cm^{-2}, and current densities ranged from 5.0 to 50.0 mA cm^{-2}.

2.4. Characterization techniques

The following techniques were used for material characterization: X-ray diffraction, Fourier transformation infrared spectroscopy, thermodifferential and thermogravimetric analyses, scanning electron microscopy, and energy dispersive X-ray analysis. The measurements were carried out by using the following instruments: Rotaflex-Rigaku model 200B diffractometer, Bomem model 102 spectrophotometer, thermal meter Netzsch STA 409, and JEOL JXA model 8900RL equipped with an energy dispersive X-ray detector.

3. Results and discussions

3.1. Anode material chemical recycling

A typical X-ray diffraction spectrum of the synthesized material at 8.0 and 25 °C is shown in Fig. 1. In comparison with the JCPDS card number 31–0228 [15], it was verified that cadmium hydroxide had a hexagonal structure. The temperature change has no influence in the cadmium hydroxide phases. The γ-$Cd(OH)_2$ phase is less stable than β-$Cd(OH)_2$, therefore, γ-$Cd(OH)_2$ became β-$Cd(OH)_2$. This material can be reused for recycled electrode production.

FT-IR absorption spectra for cadmium hydroxide were made to complement the X-ray measures. A typical example of FT-IR spectra for beta nickel hydroxide presents characteristic bands for sulphate, carbonate, and adsorbed water. The presence of carbonate is ought to the open system used in the synthesis. The absorptions bands follow the attributions below [16]:

- 3637 cm^{-1} vibrational stretching of hydroxyl group in the cadmium hydroxide lattice,

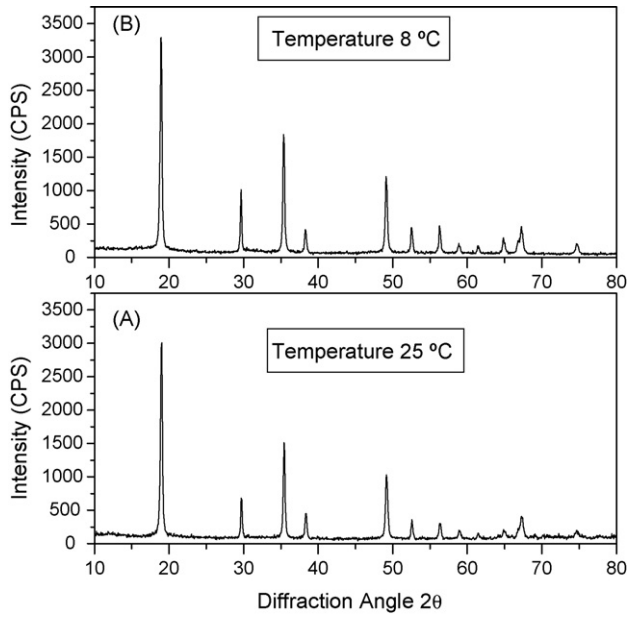

Fig. 1. Typical X-ray diffraction spectrum of the synthesized material at: (A) 25 °C; (B) 8.0 °C.

- 3427 cm^{-1} vibrational stretching of hydroxyl group of the adsorbed water,
- 1626 cm^{-1} water angular deformation,
- 1384 cm^{-1} and at 1046 cm^{-1} carbonate anion vibration stretching,
- 1137 and 922 cm^{-1} sulphate anion,
- 527 cm^{-1} water angular deformation on the plane,
- 457 cm^{-1} Cd–O vibrational stretching,
- 348 cm^{-1} water angular deformation off the plane.

In Fig. 2 a typical thermogravimetric (TDA) and thermodifferential (TDA) plots for β-$Cd(OH)_2$ can be seen. The loss mass relative percentual is plotted against the temperature increase. There is an interval of temperature where a significant loss

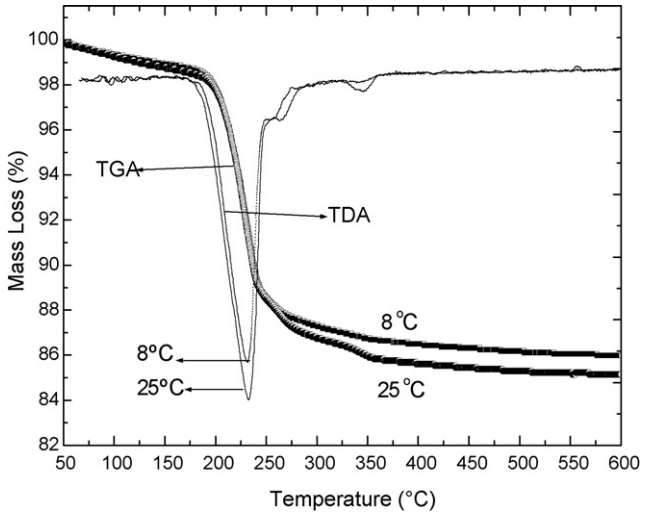

Fig. 2. Thermogravimetric (TDA) and thermodifferential (TDA) plots for β-$Cd(OH)_2$.

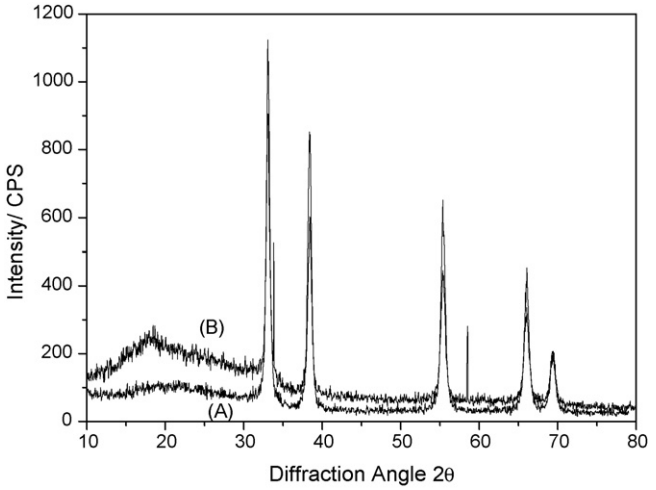

Fig. 3. Typical X-ray diffraction spectrum of the cadmium oxide formed after the thermic measures: (A) material synthesized at 25 °C; (B) material synthesized at 8 °C.

of mass can be detected. It is the range from 200 to 450 °C. In the thermodifferential (TDA) plot for cadmium hydroxide, one endothermic peak could be seen in a temperature interval between 200 and 450 °C. The thermodifferential plot is in quite agreement with the thermogravimetric one. It was verified in comparison with the JCPDS card number 05–0640 [17] that cadmium oxide is formed after the thermic measures, as it is shown in Fig. 3. There is no characteristic band for sulphate and carbonate anions on the FT-IR absorption cadmium oxide spectra. Therefore, according to the thermogravimetric, thermodifferential, X-ray diffraction, and infrared spectroscopy, the solid state reaction in the range from 200 to 450 °C corresponds to deshydroxilation reaction: $Cd(OH)_2 \rightarrow CdO + H_2O$ and the desorptions of sulphate and carbonate anions. CdO calcination happened in the temperature range between 450 and 600 °C, before the powder sintering beginning. Chemical composition for synthesized cadmium hydroxide can be expressed as follows:

$$[\beta\text{-}Cd(OH)_2(H_2O)_X(SO_4{}^{2-})_U(CO_3{}^{2-})_W]$$

where X, U, and W are the amount of substance (mol) for adsorbed H_2O, $SO_4{}^{2-}$, and $CO_3{}^{2-}$, respectively.

3.2. Electrochemical recycling of anode material

Cadmium was recovered from leaching solution using a galvanostatic technique. As the leaching solution is acidic, the reduction of the acid in the work electrode also happens. The reduction potential of the acid is smaller than that of the Cd^{2+}. Therefore, the reduction of the acid should happen first, and the reduction of Cd^{2+} should be disfavored [18]. However, in practice this was not verified. There is an anomalous electrodeposition. The density of the applied current affects the electron concentration in the metal. For low current densities, the electron level in the metal is the same as the electron level of the void orbital of ionic cadmium in the solution. As a result, the electron transfer from the metal to ionic cadmium in the solu-

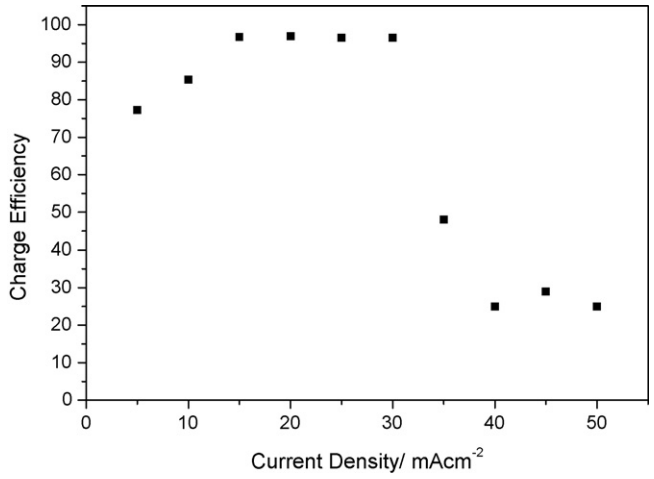

Fig. 4. Charge efficiency in function of the current density for cadmium electrodepostition in acidic solutions, 25 °C, without stirring, $q_{applied} = 90.0\,C\,cm^{-2}$.

tion happens. The increase in the current density provokes an increase to the electron level in the metal. In this case, the reduction reaction of ionic cadmium can happen in the solution, either water or acid. With a further increase in the current density, either the reduction reaction in water or acid predominates. As a result, the charge efficiency ($\alpha = q_{deposition}/q_{applied}$ where q = charge density) is larger for a current density between 15.0 and 30.0 mA cm^{-2} around 95.0% and decreases with the increase to the current density, as shown in Fig. 4. Fig. 5 presents the chronopotentiometric plot for different current densities. In the chronopotentiometric plot, the nucleation stage is attributed to the peak potential. The porosity of the electrode increases with the electrodeposition time. Therefore, current density decreases with time. As a result, the potential reaction also decreases. The reaction potential is stabilized on the first plateau of the chronopotentiometric plot for a current density between 10.0 and 29.4 mA cm^{-2}. The charge density of the first plateau potential decreased with the increase in the current density. This behavior also was observed for nickel reduction from acidic solution [19]. Either the reduction reaction of ionic cadmium or the evolution of hydrogen happened on the cadmium substrate when the electrode surface was covered with at least a monolayer of cadmium. This occurred as the deposition time increased. With the increase in electrodeposition time, the potential became low cathodic and stabilized on a second plateau. At this second plateau potential, the evolution of hydrogen on the cadmium electrode was the principal reaction for current densities over 30.0 mA cm^{-2}. For current densities over 30.0 mA cm^{-2}, a transient potential in the chronopotentiometric plots was observed as soon the current was applied. This transient potential was associated with the evolution of hydrogen and the formation of active sites by nucleation. Current density decreased with the increase in electrode porosity. As a result, the potential led to low cathodic values with increase of the electrodeposition time.

The density of the applied current affects not only the charge efficiency but also the morphology of the deposit. Fig. 6 shows the deposit micrographs. For a current density equal to 10.0 mA cm^{-2}, the crystals growth rate perpendicular to the

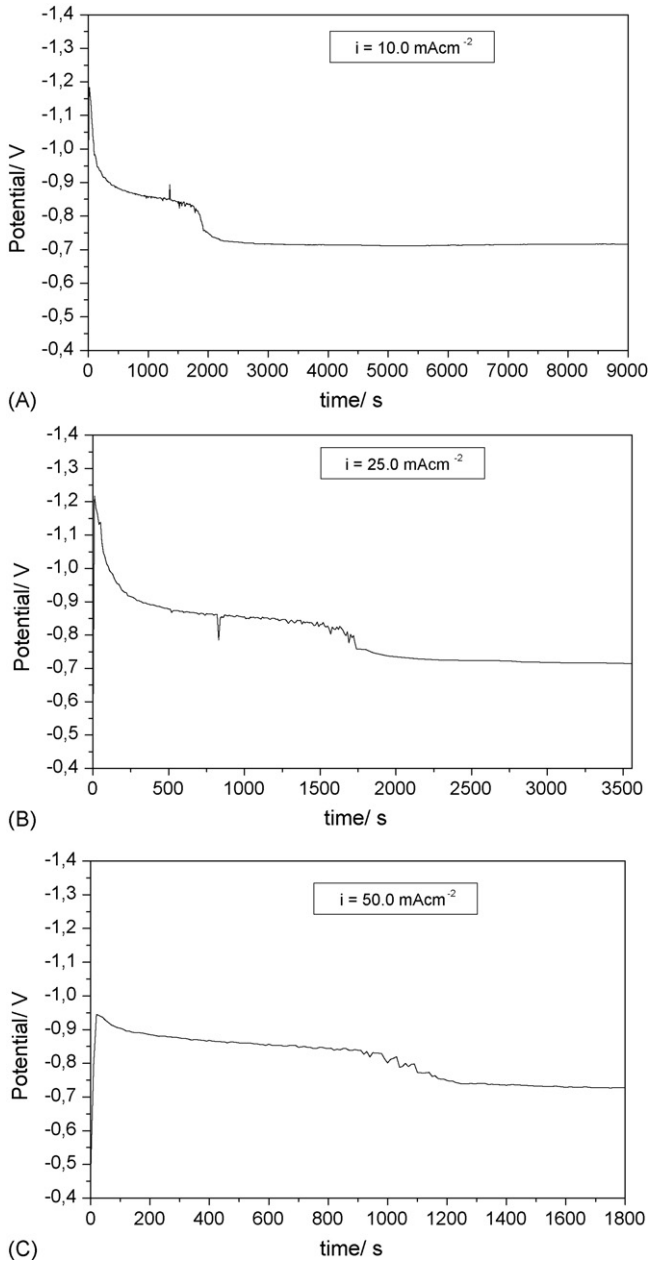

Fig. 5. Chronopotentiometric plot for ionic cadmium electrodeposition in acidic solutions, H_2SO_4 0.5 mol l^{-1}, without stirring, $q_{applied} = 90.0\,C\,cm^{-2}$. (A) $i = 10.0$ mA cm^{-2}; (B) $i = 25.0$ mA cm^{-2}; (C) $i = 25.0$ mA cm^{-2}.

electrode surface is more than in other directions. Therefore, there is a correlation between current density and coating morphology. For a current density equal to 50.0 mA cm^{-2}, the crystals growth rate in parallel direction to the electrode surface is larger than those in other directions. For a current density equal to 50.0 mA cm^{-2}, the agglomerates are more homogeneous than those formed at 10.0 mA cm^{-2}. Now, the deposits formed with current densities equal to 25.0 mA cm^{-2} possess an intermediate morphology.

To complement the characterization of the electrode surface, energy dispersive X-ray measures of the deposits formed with different current densities were made. Besides cadmium, the presence of iron is also observed in the spectra as shown in

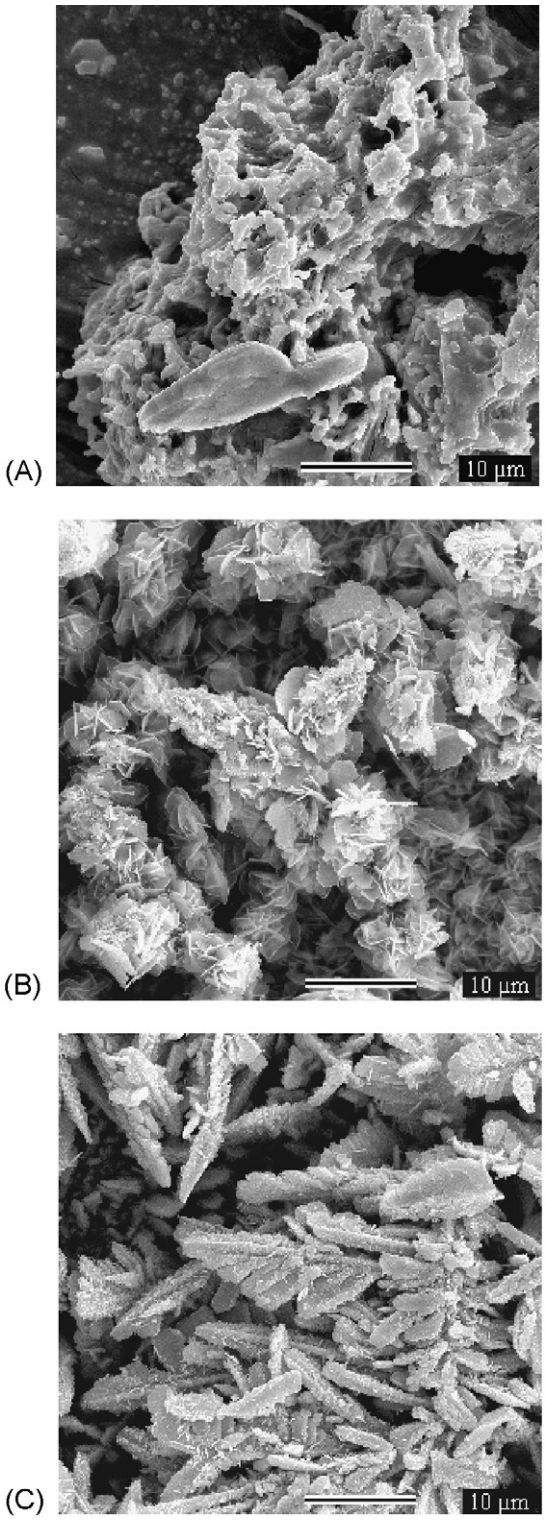

Fig. 6. Typical scanning electron microscopy for cadmium electrodeposited in acidic solutions, 25 °C, without stirring, $q_{applied} = 90.0\,C\,cm^{-2}$. (A) $i = 10.0\,mA\,cm^{-2}$; (B) $i = 25.0\,mA\,cm^{-2}$; (C) $i = 25.0\,mA\,cm^{-2}$.

Fig. 7. In the EDX spectra, it is also possible to see the presence of sulphur and oxygen derived from the deposition solution. The steel 1020 substratum is exposed due to the high microporosity of the deposits. The exposure of the substratum surface was also analyzed in the EDX spectra.

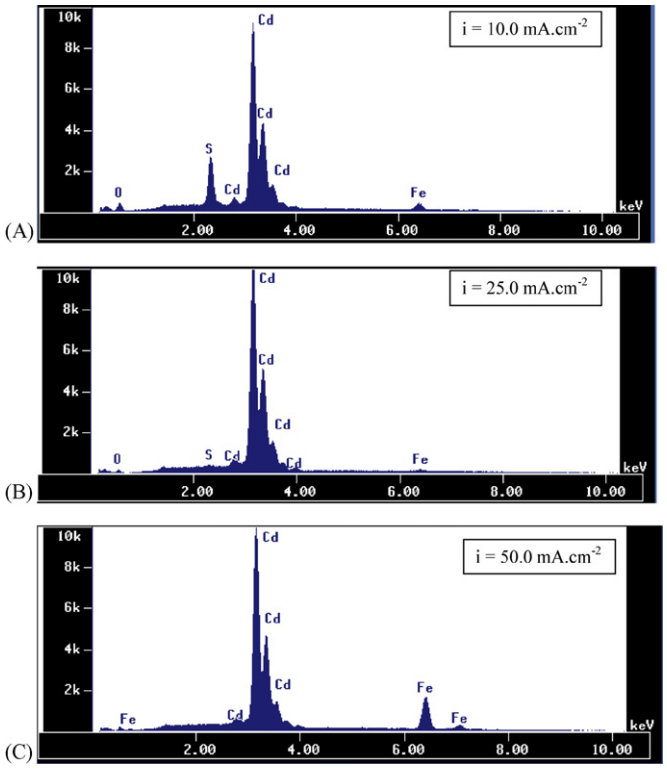

Fig. 7. Energy dispersive analysis of X-ray for cadmium electrodeposited in acidic solutions, 25 °C, without stirring, $q_{applied} = 90.0\,C\,cm^{-2}$. (A) $i = 10.0\,mA\,cm^{-2}$; (B) $i = 25.0\,mA\,cm^{-2}$; (C) $i = 25.0\,mA\,cm^{-2}$.

4. Conclusions

In this work, cadmium from Ni–Cd batteries was recycled by chemical precipitation and electrodeposition. The chemical precipitation recycling of cadmium as a precursor material was carried out at two different temperatures. It was observed through X-ray diffraction that phase β-$Cd(OH)_2$ stabilized with synthesis at 281 and 295 K. α-$Cd(OH)_2$ initially formed was transformed to β-$Cd(OH)_2$ by aging process. Chemical composition for cadmium hydroxide is:

$$[\beta\text{-}Cd(OH)_2(H_2O)_X(SO_4^{2-})_U(CO_3^{2-})_W]$$

where X, U, and W are the amounts of substance for H_2O, SO_4^{2-}, and CO_3^{2-}, respectively. The chronopotentiometric measurements presented a peak potential that indicates a nucleation stage proceeding deposit growth. The largest charge efficiency was reached for a current density between 15.0 and 30.0 $mA\,cm^{-2}$, around 95%. The current density influences the morphology of the deposits. Scanning electron microscopy showed that the cadmium deposit presents a larger microporosity for a current density equal to 10.0 $mA\,cm^{-2}$ than for 50.0 $mA\,cm^{-2}$. The deposits formed with current density equal to 25.0 $mA\,cm^{-2}$ possess an intermediate morphology. In the EDX spectra, it is also possible to observe the presence of iron of the substrate, cadmium, sulphur, and oxygen, which may have derived from the deposition solution.

Acknowledgement

The authors acknowledge PRPPG-UFES, CNPq for the financial support

References

[1] C.J. Rydh, M. Karlström, Resour. Conserv. Recycl. 34 (2002) 289.
[2] C.J. Rydh, B. Svärd, Sci. Total Environ. 302 (2003) 167.
[3] A.M. Bernardes, D.C.R. Espinosa, J.A.S. Tenório, J. Power Sources 130 (2004) 291.
[4] Y. Morioka, S. Narukawa, T. Itou, J. Power Sources 100 (2001) 107.
[5] N. Simic, R. Sjövall, U. Palmqvist, E. Ahberg, J. Power Sources 94 (2001) 1.
[6] H. Zhang, X. Ma, Y. Ji, J. XU, D. Yang, Mater. Lett. 59 (2005) 56.
[7] M.P. Waalkes, J. Inorg. Biochem. 79 (2000) 241.
[8] M. Bartolozzi, G. Braccini, S. Bonvini, P.F. Marconi, J. Power Sources 55 (1995) 247.
[9] P. Ammann, J. Power Sources 57 (1995) 41.
[10] D.C.R. Espinosa, J.A.S. Tenório, J. Power Sources 157 (2006) 600.
[11] B.R. Reddy, D.N. Pryla, S.V. Rao, P. Radhila, Hydrometallurgy 77 (2005) 253.
[12] B.R. Reddy, D.N. Pryla, K.H. Park, Sep. Purif. Technol. 50 (2006) 161.
[13] C.A. Nogueira, F. Delmas, Hydrometallurgy 52 (1999) 267.
[14] M.B.J.G. Freitas, S.F. Rosalém, J. Power Sources 139 (2005) 366.
[15] Joint Committee on Power Diffraction Standards (JCPDS), Card No. 31-0228.
[16] K. Nakamoto, Infrared and Raman Spectra of Inorganic and Coordination Compounds, Wiley & Sons, New York, 1986.
[17] Joint Committee on Power Diffraction Standards (JCPDS), Card No. 05-0640.
[18] K.J. Vetter, Electrochemical Kinetics: Theorical and Experimental Aspects, first ed., Academic Press, New York, 1967, pp. 282–327.
[19] M.B.J.G. Freitas, R.K.S. Silva, A. Rozário, J. Power Sources 158 (2006) 754.